Turkish Journal of Chemistry

http://journals.tubitak.gov.tr/chem/

Research Article

Turk J Chem
(2017) 41: 862 – 873

doi:10.3906/kim-1701-37

Investigation of photoinduced polymerization of doxycycline-imprinted hydrogels: effect of template on initiator reactivity, conversion, and reaction rate

Dilek DALGAKIRAN[1], Tuğçe İNAN[2], Fatma Seniha GÜNER[2,*]
[1]Program of Polymer Science and Technology, İstanbul Technical University, Maslak, İstanbul, Turkey
[2]Department of Chemical Engineering, Faculty of Engineering, İstanbul Technical University, Maslak, İstanbul, Turkey

Received: 20.01.2017 • **Accepted/Published Online:** 31.05.2017 • **Final Version:** 20.12.2017

Abstract: Photopolymerization kinetics of doxycycline hyclate (DOX)-imprinted hydrogels were monitored by real-time Fourier transform infrared spectroscopy and differential photocalorimetry. 2-Hydroxyethyl methacrylate-based hydrogels were synthesized by using ethylene glycol dimethacrylate as a cross-linker, acrylic acid (AA) as a functional monomer, and 2,2-dimethyl-2-hydroxy acetophenone as a photoinitiator. For imprinting DOX in hydrogels, the molar ratio of template to functional monomer (DOX:AA) was chosen as 1:8 and 1:16. The polymerization was achieved at two different initiator concentrations. The conversion and reaction rate were calculated as a function of the molar ratio of template, and the results were compared to those of nonimprinted ones. In order to reveal the effect of DOX on the photoinduced radical polymerization, thermal polymerization was also performed for imprinted and nonimprinted hydrogels by using 2,2′-azobis(2,4-dimethyl-pentanenitrile) as a thermal initiator. All results showed that there is a significant effect of DOX concentration on the conversion and reaction rate of the photopolymerization reaction. The conversion and reaction rate decreased during photopolymerization when the template concentration increased in the monomer mixture.

Key words: Molecular imprinting, photopolymerization, photosensitivity

1. Introduction

Molecular imprinting is a technique used to recognize molecules with special binding sites, and thus it allows to develop new materials for separation processes,[1] controlled release drug delivery systems,[2] recognition of molecules,[3] selective adsorbents,[4] solid-phase extraction,[5] and chemical sensors[6] The main factors for designing imprinted polymers are polymerization methods (UV or heat),[7] structures of template molecules, functional monomers and cross-linkers, molar ratio of template to functional monomer,[8–12] reaction temperature,[13] pressure,[14] and stochiometry[15] Functional groups such as –C = O and –OH coming from the monomer are involved in intermolecular hydrogen bonding in the presence of proton acceptors, i.e. oxygen and nitrogen from the template molecule.[8] The formation of a stable complex between the template and functional monomer can be achieved by adjusting the reaction conditions.[7] Previous studies showed that if thermal initiation is applied for free radical polymerization, the temperature should be as low as possible for a successful imprinting performance. For this reason, photopolymerization is widely preferred in molecular imprinting processes. However, properties of the template molecule should be considered with priority when the reaction type and/or initiator is chosen. There are numerous studies about preparation of molecular imprinting polymers and a few studies are about

*Correspondence: guners@itu.edu.tr

investigation of the effect of the template concentration on the polymerization kinetics for molecular imprinted polymers.[16,17] These studies explained the influence of template–monomer interactions on monomer conversion and reaction rate for imprinted polymers. Our research is related to the effect of template concentration on the reactivity of the initiator, conversion, and overall reaction rate for imprinted hydrogels.

2-Hydroxy-2-methyl-1-phenyl-propan-1-one is widely used as a photoinitiator to initiate acrylates in combination with other monomers (mono- or multifunctional).[18−20] After excitation with light, the excited initiator creates radicals to initiate polymerization reaction. The efficiency of an initiator depends on a number of factors.[21] One factor that influences radical generation is a good association between the absorption spectrum of the initiator and the emission spectrum of the light source for high absorptivity.[22,23] The second factor that has an important effect on radical generation is initiator concentration. Studies showed that there is an upper limit for initiator concentration. Above this concentration, the final conversion is not enhanced by increasing initiator concentration. Besides these factors, competitive cases can deactivate radical generation; radical formation is restricted by oxygen, additives, or monomer.[24,25]

In this study, doxycycline was chosen as a template molecule for preparation of imprinted hydrogels. It is a synthetic broad-spectrum antibacterial tetracycline (TC) derivative antibiotic (Figure 1) and doxycycline hyclate is the most widely used form for several purposes.[26] In the literature, TC-based imprinted polymers were also prepared for chromatographic evaluations,[27] solid-phase extractions,[28] and affinity membranes.[29]

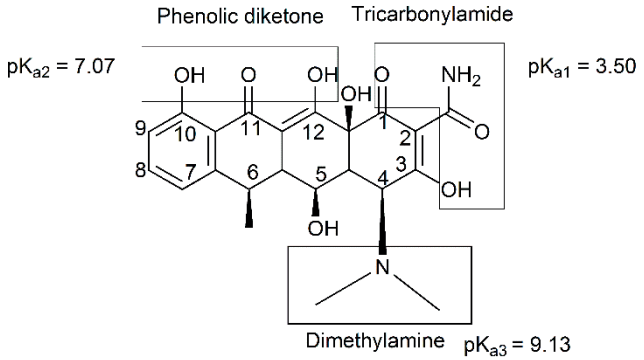

Figure 1. Chemical structure of the doxycycline.

Although there are many benefits of doxycycline, a significant problem for doxycycline usage for medical purposes is its photosensitivity.[30] The photolysis of doxycycline under UVC light (100–280 nm) was investigated by Bolobajev et al. It was reported that degradation of doxycycline occurred under various conditions.[31] Although many studies about skin irritation by doxycycline under sunlight have been presented in the literature,[30,32,33] there is no scientific study investigating the effect of doxycycline degradation on initiator reactivity, reaction rate, and conversion during UV-initiated free radical polymerization.

Our aim is to prepare doxycycline hyclate (DOX)-imprinted hydrogel films for treatment of corneal neovascularization. There are two alternative approaches for the synthesis of imprinted hydrogels: thermal polymerization and photopolymerization. While there are no studies clarifying the effect of template molecules on initiator reactivity, conversion, and reaction rate related to the polymerization method, we designed preliminary studies for choosing an alternative reaction method. The conversion and reaction rate in the photopolymerization reaction of imprinted hydrogels were determined in various doxycycline moieties at a constant ratio of functional monomer to cross-linker. The polymerization reaction was initiated with either a photo- or thermal

initiator, and the results were compared. The isothermal reaction kinetic was studied by Fourier transform infrared (FTIR) spectroscopy and differential photocalorimetry (DPC). The obtained data will be used for a further study that targets the preparation of contact lenses from doxycycline-imprinted hydrogels for treatment of corneal neovascularization.

2. Results and discussion

The effects of the template amount on the conversion and reaction rate were investigated for the doxycycline-imprinted hydrogels. It was reported in the literature that there is no significant degradation of doxycycline molecules at 40 °C over a period of 30 days,[34] so the thermal polymerization occurred at 45 °C in an oven. For the UV-initiated reaction, in order to obtain maximum conversion, the reaction mixture was placed into an oven at 40 °C for 16 h for post curing. The conversions were calculated for both nonimprinted and imprinted hydrogels for each UV- and thermal-initiated reactions.

2.1. Determination of monomer conversion by real-time FTIR

The conversion of monomers was determined by real-time FTIR. The FTIR spectra for the synthesis of nonimprinted hydrogels are given in Figure 2 as an example.

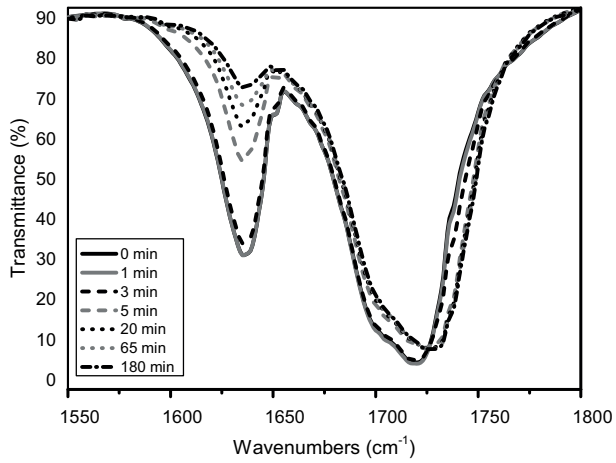

Figure 2. FTIR spectra of the reaction mixture of NIP-l-P coded hydrogel at different time intervals during the photopolymerization.

The height of the peak at about 1635 cm^{-1} decreased with reaction time. The reaction was completed in 10–20 min for low initiator concentrations and 2–10 min for high initiator concentrations. The conversion calculated from FTIR data can be seen in Figures 3 and 4. Eq. (1) was used to calculate the conversion:

$$Conversion\ (\%) = \left(1 - \frac{A_{hydrogel\ 1635\,cm-1}/A_{hydrogel\ 1719\,cm-1}}{A_{monomer\ 1635\,cm-1}/A_{monomer\ 1719\,cm-1}}\right) \times 100\,, \tag{1}$$

where A is the height of the peak at 1635 or 1719 cm^{-1} for the reaction mixture.

Table 1 shows the overall results for conversion of imprinted and nonimprinted hydrogels prepared by photopolymerization in relatively low (l) and high (h) initiator concentration at 25 °C.

In general, it is expected that increasing the concentration of initiator in a hydrogel increases the rate of polymerization and the overall monomer conversion. According to our results, the highest conversion was

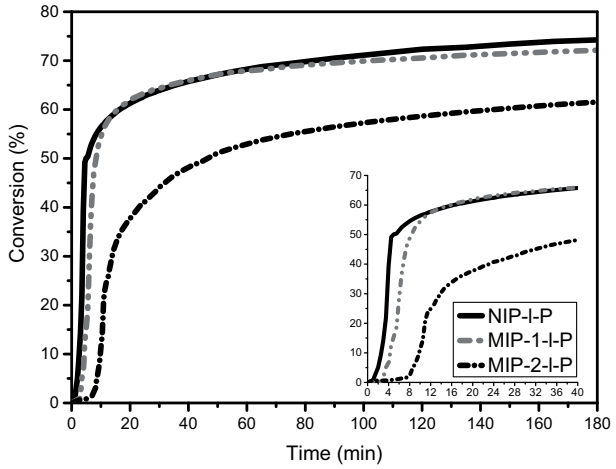

Figure 3. Conversion of double bonds as a function of time from FTIR data for low initiator ratio.

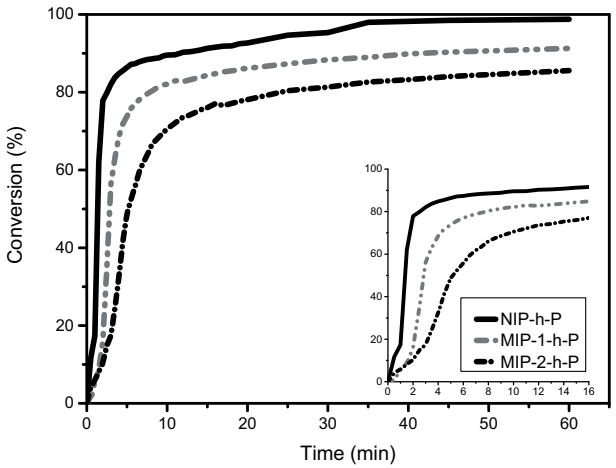

Figure 4. Conversion of double bonds as a function of time from FTIR data for high initiator ratio.

Table 1. Conversions calculated from FTIR data.

Code	Conversion (%)			
	UV(1h)	UV(3h)	UV(3h) + Thermal(16h)	Thermal
NIP-l-P	68.8	74.3	82.0	
MIP-1-l-P	68.2	72.1	74.9	-
MIP-2-l-P	53.8	61.5	69.6 (70.1*)	-
NIP-h-P	98.8	-	-	-
MIP-1-h-P	91.3	-	-	-
MIP-2-h-P	85.6	-	-	-
NIP-l-T	-	-	-	86.4
MIP-1-l-T	-	-	-	88.1
MIP-2-l-T	-	-	-	84.5

*After 60 h (3 h under UV light + 57 h in oven).

achieved in a high initiator concentration in the absence of doxycycline (NIP-h-P). The MIP-2-l-P coded sample, which has the highest amount of doxycycline in the reaction mixture in the series of low initiator concentrations, gave the lowest conversion. The conversion of MIP-1-l-P was slightly lower than that of NIP-l-P, but the difference was not significant. Even though photopolymerization continued for 3 h at 365 nm and each hydrogel was placed in an oven at 40 °C for 16 h, the conversion of both MIP-1-l-P and MIP-2-l-P could not reach the same value as NIP-l-P. To promote conversion for MIP-2-l-P, the reaction mixture was also kept for 57 h at 40 °C in the oven, but no higher monomer conversion was obtained. Similar results were obtained for the high initiator concentration for the UV-initiated system. On the other hand, the conversion was almost the same for thermal polymerization performed in both the absence and presence of doxycycline. This can be attributed to the fact that DOX influences the UV-initiated polymerization negatively.

2.2. Determination of reaction rate by real-time FTIR and DPC

The rate of polymerization reaction was determined by two methods: FTIR and DPC. In Figures 5 and 6, the polymerization rate (R_p) for each hydrogel synthesized by photopolymerization is plotted as a function of time for high and low initiator concentrations. R_p is the overall reaction rate, calculated from FTIR data using Eq. (2):[35]

$$R_P = -\frac{d[M]}{dt} = \frac{[M_0] \times (A_1 - A_2)}{A_0 \times (t_1 - t_2)}, \quad (2)$$

where A_0 is the ratio of the peak heights at 1635 cm^{-1} to 1719 cm^{-1} at the beginning of the reaction, A_1 is the height of the peak at t_1, A_2 is the height of the peak at t_2, and M_0 is initial molar concentration of all monomers in the reaction mixture.

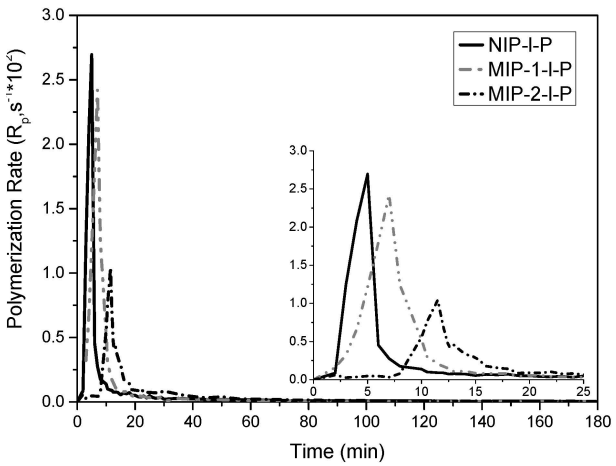

Figure 5. Polymerization rate as a function of time from FTIR data in low initiator ratio.

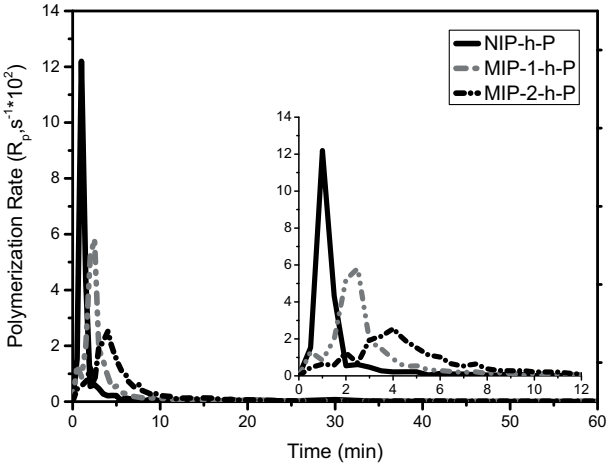

Figure 6. Polymerization rate as a function of time from FTIR data for high initiator ratio.

The heat flow of the reaction mixture for NIP-1-P, MIP-1-l-P, and MIP-2-l-P was obtained by DPC and the polymerization rate calculated from Eq. (3) is presented in Figure 7.

$$R_P = \frac{H/W}{\Delta H} \quad (3)$$

Here, R_p is the polymerization rate (s^{-1}), H is the heat flow (mW), W is the weight of the monomer mixture (g), and ΔH is the enthalpy of the material (J/g).[16]

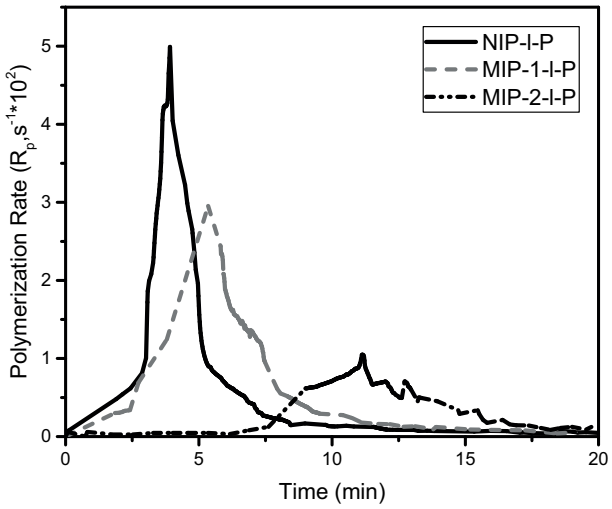

Figure 7. Polymerization rate as a function of time from DPC data for low initiator ratio.

The rates of polymerization reactions obtained from both FTIR and DPC data for MIP-coded samples were calculated to be lower than those of NIP-coded samples for each series. When the amount of DOX increased from 1.33×10^{-5} to 2.66×10^{-5} mol, the polymerization rate decreased for both high and low initiator concentrations. Additionally, the induction time shifted to a longer time with increasing amounts of DOX in the reaction mixture due to a higher deactivation effect of DOX with higher molar ratios (Figures 5–7).

The obtained results for conversion and overall reaction rate can be explained by the chemical structure and sensitivity of the DOX against UV radiation. It can be clearly seen that DOX has an influence on the polymerization system. For each specific hydrogel composition, the conversions of imprinted and nonimprinted systems had significantly different values. The effect of the DOX on initiator reactivity can also be seen more specifically from overall reaction rate results. Unexpectedly, the reaction rate and the conversion of the imprinted hydrogels did not reach the values of the nonimprinted ones. In the literature, the effect of template–monomer interaction on polymerization reaction has been reported by a few researchers.[16,36] These studies indicated that template–monomer interactions cause an initial decrease for imprinted hydrogel polymerization; at the end of the polymerization, both conversion and reaction rate are similar for all hydrogels. We thus realized that there are some different factors that affect the polymerization reaction in the presence of DOX.

A reaction pathway is proposed for restriction of radical generation in Scheme 1. DOX absorbs UV radiation at a higher wavelength than the photoinitiator; therefore, the excitation of the initiator cannot occur alone.[24] While the initiator has λ_{max} at 322 nm, the $\lambda_{\max}$ for DOX appears at 345 nm. However, $\lambda_{\max}$ values for these components were not at same wavelengths; they were adjacent molecules in the ground state. It was proposed that DOX was likely to be hindering radical generation by the photoinitiator and therefore the overall conversion and the reaction rate decreased. DOX acted as a UV absorber against the photoinitiator. As reported in the literature it is indicated that some additives such as pigments in a composition damage the light absorption of the initiator.[37,38] DOX molecules absorb UV energy at a higher wavelength than the initiator; it causes the blocking of generation of active radicals to form RM., to decrease the radical generation rate with absorbing UV light. Restriction of the initiator at ground state is an unfavorable situation due to hindering the generation of monomeric radicals, RM., reducing initiator efficiency. The number of active radicals produced per photon of light absorbed is restricted by absorbing UV light.[38]

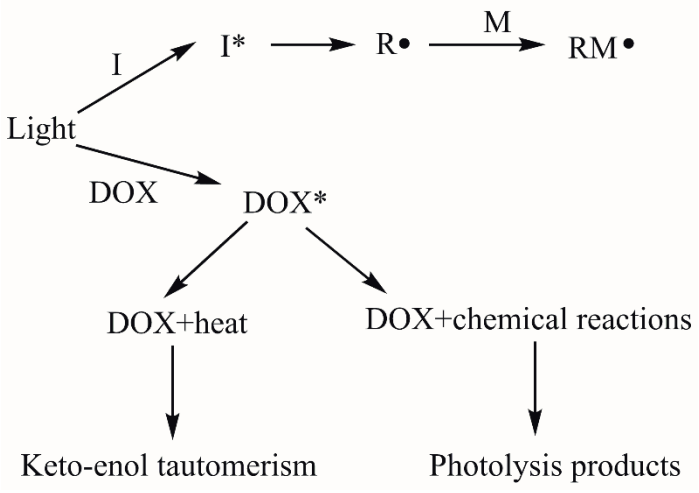

Scheme 1. Schematic representation of the reaction mechanism for the photoinitiator and DOX structure.

It is explained in the literature that exposure to the light causes the photoactivation of drugs that have chromophore groups (a radiation-absorbing substance). Most commonly, wavelengths within the UVA spectrum (320–400 nm) cause drug-induced photosensitivity reactions. Mostly, they have at least one resonating double bond or an aromatic ring that can absorb UV energy. In many examples, photoactivation of a chemical ensues with the excitation of electrons from the stable singlet state to an excited triplet state. The excited state converts into a more stable state with two different pathways for DOX.[37,38]

The excess energy disappears as heat. DOX has a conjugated phenolic diketone group at position 10–12, which causes keto-enol tautomerization.[39,40] When DOX absorbs the UV light, it is possible to dissipate the absorbed energy as heat via an exited state keto-enol tautomerism like a UV absorber (Scheme 2).[41] It is obvious that different tautomeric species are present in the reaction mixture with different moieties. All tautomers in their different conformations interact with the functional monomer during polymerization. The template–monomer interactions are destroyed due to tautomeric conversions.

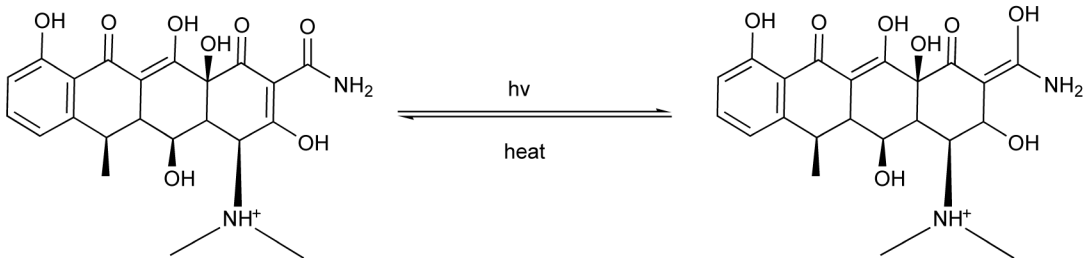

Scheme 2. Keto-enol tautomerism of DOX.

Chemical reaction(s) may occur depending upon the chemical structure of the molecule. The molecule uses the energy of excitation to undergo a chemical reaction. Photolysis is the most substantial process in the degradation of the antibiotic and induced by solar irritation. Degradation with photolysis can be realized in two ways: direct and indirect. In direct degradation which is our case, the UV radiation is absorbed by the drug molecule and byproducts are produced. In the case of indirect degradation, strong oxidizing radicals are generated by natural components and these radicals react with drug molecules.[42] Jiao et al. indicated that the positively charged tetracycline (TC^+) form of TC molecules substantially inhibited photolysis and, contrary to this, the TC^0 form encouraged photolysis.[43] Protonation states of the TC give information about the stability of the structure in media with different pH values. It was also demonstrated that TC had low stability at high pH values. Negatively charged drug molecules tend to interact with active radicals; therefore, strong electrical density of the ring structure causes photodegradation of TCs.[43] In our study the reaction medium was at about pH 3. In this condition, DOX is present in the monomer mixture in the $DOXH_3^+$ form, so it is estimated that the DOX degradation rate is low even though UV energy absorption occurs during the molecular imprinting photopolymerization at 365 nm (Eqs. (4)–(6), adapted from Jiao et al.[43]).

$$DOXH_3^+ \leftrightarrow DOXH_2^0 (pK_{a1} = 3.50) \tag{4}$$

$$DOXH_2^0 \leftrightarrow DOXH^- (pK_{a2} = 7.07) \tag{5}$$

$$DOXH^- \leftrightarrow DOX^{2-} (pK_{a3} = 9.13) \tag{6}$$

In our study, DOX molecules are excited in association with the initiator. In light of the explanations summarized above, it is assumed that photolysis reactions occur during polymerization. It is expected in our study that the DOX degradation rate is low even though UV energy absorption occurs during the molecular imprinting photopolymerization at 365 nm.

Finally, we concluded that for preparation of DOX-imprinted hydrogels, thermal-induced polymerization is a more suitable method than the UV-initiated one.

For morphological characterization, first the imprinted hydrogels were washed with a mixture of oxalic acid : methanol : acetonitrile (65:15:20, v/v) solution for 24 h and then with methanol for 24 h to ensure the complete removal of template molecules. Scanning electron microscope (SEM) images of NIPs and MIPs are shown in Figures 8a–8d as an example. The cavities created by the template molecule via the molecular imprinting technique are seen clearly from the SEM images. The images help to provide a general idea about the morphology of hydrogels and to identify the structural differences between MIPs (Figures 8a and 8c) and NIPs (Figures 8b and 8d) in detail.

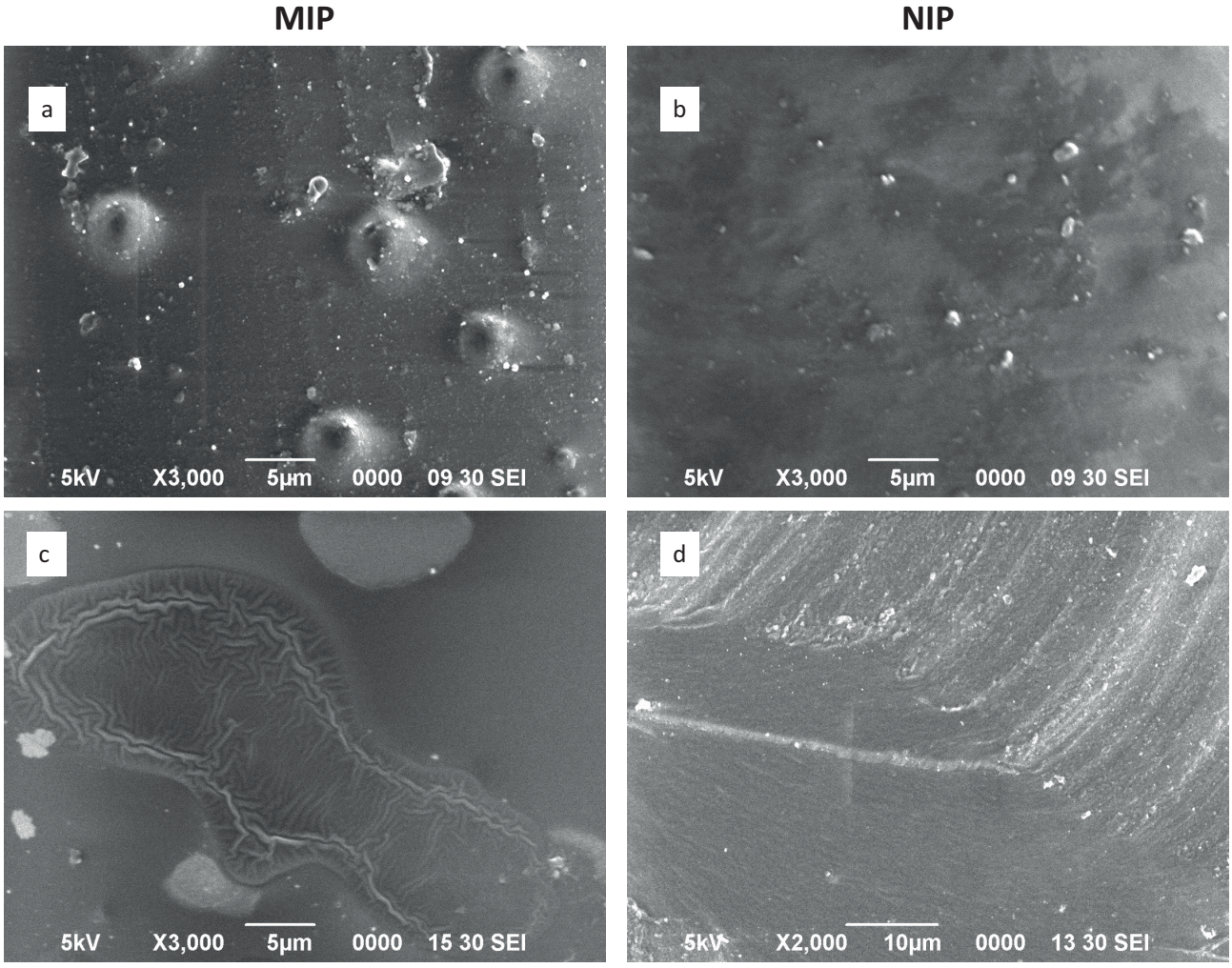

Figure 8. Representative SEM images of MIPs and NIPs prepared by thermal induced polymerization from surface (a and b) and cross-sectional area (c and d).

2.3. Conclusions

The aim of this study was to investigate the effect of template concentration on the conversion and rate of polymerization reaction for the preparation of DOX-imprinted hydrogels. In the study two measurement methods were used: real-time FTIR spectroscopy and DPC. The obtained data showed that the conversion and the overall reaction rate decreased when the template concentration increased in the reaction mixture. The highest conversion and reaction rates were obtained for the mixture of nonimprinted hydrogel. Additionally, the induction period of the polymerization shifted to a longer time with increasing concentrations of the DOX in the reaction mixture. On the other hand, the conversion and the reaction rate of the thermal polymerization were found almost the same for imprinted and nonimprinted hydrogels. These results can be taken as clarification that DOX was excited during polymerization. Tautomeric species and photolysis products of DOX may occur in the reaction medium because of its photosensitivity.

3. Experimental

3.1. Materials

Commercially available 2-hydroxyethyl methacrylate (HEMA) was purchased from Sigma Aldrich. Ethylene glycol dimethacrylate (EGDMA, Sigma Aldrich) was used as a cross-linker, acrylic acid (AA, Sigma Aldrich) as a functional monomer, 2-hydroxyl-2-methyl-1-phenyl-propan-1-one (Sigma-Aldrich) as a photoinitiator, and 2,2′-azobis(2,4-dimethylvaleronitrile) (DuPont) as a thermal initiator. DOX, used as the template molecule, was gifted by Deva (İstanbul, Turkey). Sodium chloride was purchased from Merck for preparing pellets and it was used after drying in an oven for one night at 120 °C. All other chemicals were used as received.

3.2. Synthesis of imprinted and nonimprinted hydrogels

3.2.1. Photoinduced polymerization

Molecular imprinted hydrogels (MIPs) were synthesized via free radical photopolymerization. In the imprinted polymer synthesis, 2 mL of HEMA and 14.6 μL of AA were mixed. DOX was added into the HEMA-AA mixture with two different molar ratios (1.33×10^{-5} or 2.66×10^{-5} mol) at two different amounts of initiator (8.74×10^{-5} or 4.23×10^{-4} mol). The backbone monomer, HEMA, is liquid, so no additional solvent was used. After addition of the initiator, the mixture was sonicated for 5 min and was purged with N_2 for 15 min to prevent O_2 inhibition of the initiator. Then the solution was transferred into a mold and the polymerization was initiated at 365 nm light source at room temperature.

3.2.2. Thermally induced polymerization

Similar procedures were followed for UV- and thermal-initiated polymerization reactions, but after transfer into the mold, the polymer solution was kept at 45 °C for 24 h.

Nonimprinted hydrogels (NIPs) were prepared in the absence of DOX by photo and thermal polymerization methods as comparison samples. The compositions and codes of the polymers are given in Table 2, and the schematic representation of the reaction is shown in Scheme 3.

Table 2. Molar ratios used for polymerization in the presence and absence of template molecule.

Code	Initiation type	HEMA (mL)	AA (μL)	EGDMA (μL)	Initiator (mol)	DOX (mol)	DOX : AA
NIP-l-P	Photo	2	14.6	64.3	8.74×10^{-5}	-	-
MIP-1-l-P	Photo	2	14.6	64.3	8.74×10^{-5}	1.33×10^{-5}	1:16
MIP-2-l-P	Photo	2	14.6	64.3	8.74×10^{-5}	2.66×10^{-5}	1:8
NIP-h-P	Photo	2	14.6	64.3	4.23×10^{-4}	-	-
MIP-1-h-P	Photo	2	14.6	64.3	4.23×10^{-4}	1.33×10^{-5}	1:16
MIP-2-h-P	Photo	2	14.6	64.3	4.23×10^{-4}	2.66×10^{-5}	1:8
NIP-l-T	Thermal	2	14.6	64.3	8.74×10^{-5}	-	-
MIP-1-l-T	Thermal	2	14.6	64.3	8.74×10^{-5}	1.33×10^{-5}	1:16
MIP-2-l-T	Thermal	2	14.6	64.3	8.74×10^{-5}	2.66×10^{-5}	1:8

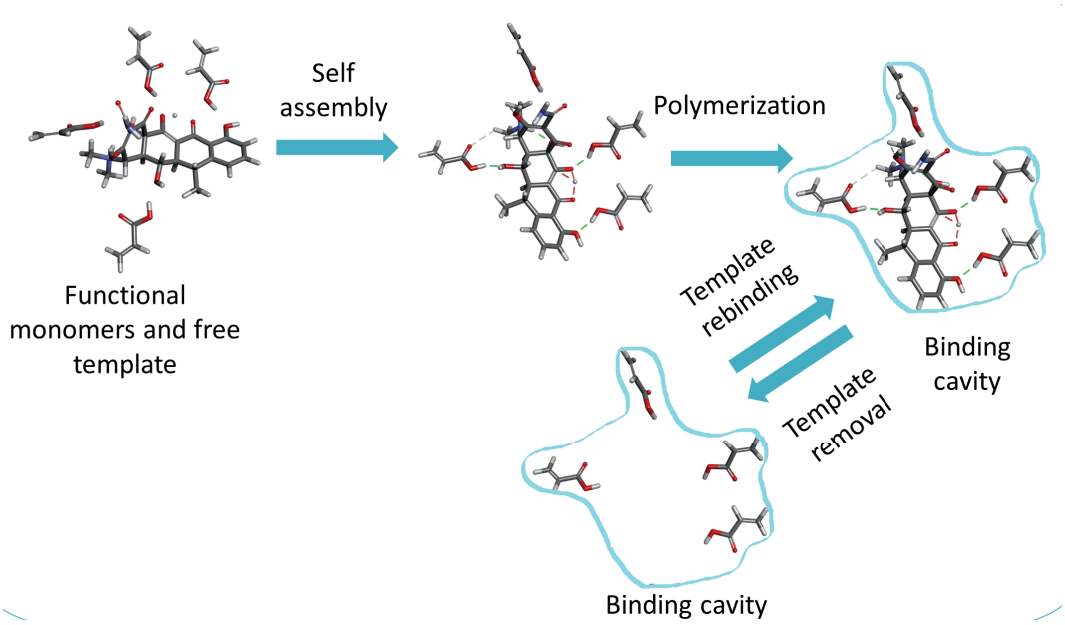

Scheme 3. Schematic representation of DOX imprinting procedure.

3.3. Monitoring of polymerization reaction

3.3.1. Fourier transform infrared spectroscopy

The polymerization reaction was monitored by real-time FTIR spectroscopy (PerkinElmer Spectrum One). In order to prevent the inhibiting effect of oxygen, the FTIR cell was purged with N_2 for 30 min before each measurement. The monomer mixture was placed between two transparent NaCl pellets and exposed to UV light. The spectral changes were recorded for a maximum of 3 h at intervals. The reaction was monitored by measuring the peak height at about 1635 cm^{-1} assigned to the C = C stretching vibration. The peak corresponding to the –C = O carbonyl bond at approximately 1719 cm^{-1} was used as an internal standard. The light intensity was 20 mW/cm^2. After the end of irradiation, the pellets were annealed at 40 °C to completion of the curing reaction and then the conversion was calculated.

3.3.2. Differential photocalorimetry

The heat flow of the reaction was recorded as a function of time during the polymerization under isothermal conditions by using a Pyris Diamond differential scanning calorimeter equipped with an EXFO Omni-Cure 2000

photo-DSC accessory (DPC, PerkinElmer). The temperature was held constant at 25 °C and N_2 was purged in order to eliminate the oxygen from the DPC cell. Both the aluminum pan filled with 8–12 mg of reaction mixture and the empty reference aluminum pan were covered with quartz covers. After stabilization of the test conditions, the light was turned on for 25 min. The area under the endothermic peak of the DPC curve was used to calculate the total heat of the reaction.

3.4. Characterization of the NIPs and MIPs by SEM

Washed and dried samples (NIPs and MIPs) were adhered to double-sided tape. The tape strips were attached to the platform of the SEM (JEOL, JSM-6390LV). Images were obtained using platinum-coated samples.

Acknowledgments

This work was funded by the Scientific and Technological Research Council of Turkey (TÜBİTAK) with project number 114M459. The authors acknowledge Dr Özlem Gürses (Dünya Göz Hospital, Ankara, Turkey) for her comments and valuable suggestions about the treatment of corneal neovascularization. The authors would also like to especially thank Deva (İstanbul, Turkey) and Assistant Professor Pelin Süzgün (Marmara University, Faculty of Pharmacy) for providing doxycycline.

References

1. Byrne, M. E. ; Salian, V. *Int. J. Pharm.* **2008**, *364*, 188-212.
2. Tieppo, A.; White, C. J.; Paine, A. C.; Voyles, M. L.; McBride, M. K.; Byrne, M. E. *J. Control. Release* **2012**, *157*, 391-397.
3. Vasapollo, G.; Del Sole, R.; Mergola, L.; Lazzoi, M. R.; Scardino, A.; Scorrano, S.; Mele, G. *Int. J. Mol. Sci.* **2011**, *12*, 5908-5945.
4. Yu, Q.; Deng, S.; Yu, G. *Water Res.* **2008**, *42*, 3089-3097.
5. Andersson, L. I. *J. Chromatogr. B Biomed. Sci. Appl.* **2000**, *739*, 163-173.
6. Kriz, D.; Ramström, O.; Mosbach, K. *Anal. Chem.* **1997**, *69*, 345A-349A.
7. Yan, H.; Row, K. H. *Int. J. Mol. Sci.* **2006**, *7*, 155-178.
8. Karim, K.; Breton, F.; Rouillon, R.; Piletska, E. V.; Guerreiro, A.; Chianella, I.; Piletsky, S. A. *Adv. Drug Deliv. Rev.* **2005**, *57*, 1795-1808.
9. Spivak, D. A. *Adv. Drug Deliv. Rev.* **2005**, *57*, 1779-1794.
10. Wei, S.; Mizaikoff, B. *J. Sep. Sci.* **2007**, *30*, 1794-1805.
11. Martin-Esteban, A. *Fresenius J. Anal. Chem.* **2001**, *370*, 795-802.
12. Cormack, P. A. G.; Elorza, A. Z. *J. Chromatogr. B* **2004**, *804*, 173-182.
13. Sellergren, B.; Shea, K. J. *J. Chromatogr. A* **1993**, *635*, 31-49.
14. Sellergren, B.; Dauwe, C.; Schneider, T. *Macromolecules* **1997**, *30*, 2454-2459.
15. Andersson, L. I.; Müller, R.; Vlatakist, V.; Mosbach, K. *P. Natl. Acad. Sci. USA* **1995**, *92*, 4788-4792.
16. Oral, E.; Peppas, N. A. *Polymer* **2004**, *45*, 6163-6173.
17. Venkatesh, S.; Sizemore, S. P.; Byrne, M. E. *Biomaterials* **2007**, *28*, 717-724.
18. Hiratani, H.; Alvarez-Lorenzo, C. *Biomaterials* **2004**, *25*, 1105-1113.
19. Hiratani, H.; Alvarez-Lorenzo, C. *Langmuir* **2002**, *83*, 223-230.

20. White, C. J.; McBride, M. K.; Pate, K. M.; Tieppo, A.; Byrne, M. E. *Biomaterials* **2011**, *32*, 5698-5705.
21. Leach, J. H. MSc, Virginia Polytechnic Institute and State University, Blacksburg, VA, USA, 2003.
22. Schneider, L. F. J.; Pfeifer, C. S. C.; Consani, S.; Prahl, S. A.; Ferracane, J. L. *Dent. Mater.* **2008**, *24*, 1169-1177.
23. Jakubiak, J.; Sionkowska, A.; Lindén, L. A.; Rabek, J. F. *J. Therm. Anal. Calorim.* **2001**, *65*, 435-443.
24. Fouassier, J. P.; Allonas, X.; Burget, D. *Prog. Org. Coatings* **2003**, *47*, 16-36.
25. Stansbury, J. W. *J. Esthet. Dent.* **2000**, *12*, 300-308.
26. Van Boeckel, T. P.; Gandra, S.; Ashok, A.; Caudron, Q.; Grenfell, B. T.; Levin, S. A.; Laxminarayan, R. *Lancet Infect. Dis.* **2014**, *14*, 742-750.
27. Jing, T.; Gao, X. D.; Wang, P.; Wang, Y.; Lin, Y. F.; Zong, X. C.; Zhou, Y. K.; Mei, S. R. *Chinese Chem. Lett.* **2007**, *18*, 1535-1538.
28. Yang, C.; Zhang, Z.; Chen, S.; Yang, F. *Microchim. Acta* **2007**, *159*, 299-304.
29. Suedee, R.; Srichana, T.; Chuchome, T.; Kongmark, U. *J. Chromatogr. B Anal. Technol. Biomed. Life Sci.* **2004**, *811*, 191-200.
30. Yong, C. K. K.; Prendiville, J.; Peacock, D. L.; Wong, L. T. K.; Davidson, A.G. F. *Pediatrics* **2000**, *106*, e13.
31. Bolobajev, J.; Trapido, M.; Goi, A. *Chemosphere* **2016**, *153*, 220-226.
32. Monser, L.; Darghouth, F. *J. Pharm. Biomed. Anal.* **2000**, *23*, 353-362.
33. Su, W.; Li, Z.; Lin, M.; Li, Y.; He, Z.; Wu, C.; Liang D. *Graefes Arch. Clin. Exp. Ophthalmol.* **2011**, *249*, 421-427.
34. Injac, R.; Djordjevic-Milic, V.; Srdjenovic, B. *J. Chromatogr. Sci.* **2007**, *45*, 623-628.
35. Sangermano, M.; Meier, P.; Tzavalas, S. In *Materials Science, Engineering and Technology*; Theophile, T., Ed. InTech: Rijeka, Croatia, 2012, pp. 325-336.
36. Rosa, J.; Couceiro R.; Concheiro, A. *Acta Biomaterilia* **2008**, *4*, 745-755.
37. Terrones, G.; Pearlstein, A. J. *Macromolecules* **2001**, *34*, 3195-3320.
38. Ravve, A. *Light-Associated Reactions of Synthetic Polymers*; Springer: Berlin, Germany, 2006.
39. Santos, M. M.; Silva, D. M.; Martins, F. T. A.; Legendre, O.; Azarias, L. C.; Rosa, I. M. L.; Neves, P. P.; De Araujo, M. B.; Doriguetto, A. C. *Cryst. Growth Des.* **2014**, *14*, 3711-3726.
40. Duarte, H. A.; Carvalho, S.; Paniago, E. B.; Simas, A. M. *J Pharm Sci.* **1999**, *88*, 111-120.
41. Gugumus, F. *Plastic Additives*, 3rd ed.; Hanser Publishers: Munich, Germany, 1990.
42. Borghi, A. A.; Palma, M. S. A. *Brazilian J. Pharm. Sci.* **2014**, *50*, 25-40.
43. Jiao, S.; Zheng, S.; Yin, D.; Wang, L.; Chen, L. *Chemosphere* **2008**, *73*, 377-382.